VOL. 10, NO. 5, MARCH 2015 ISSN 1819-6608
ARPN Journal of Engineering and Applied Sciences

www.arpnjournals.com

DESIGN AND ANALYSIS OF SILICON DIAPHRAGM OF A MEMS PRESSURE SENSOR

S. Maflin Shaby
Department of Electronics and Telecommunication Engineering, Sathyabama University, Chennai, India
E-Mail: maflin.s@gmail.com

ABSTRACT

Pressure measurements in industries, biomedical and marine environment are of utmost importance to better understand the process stability, ocean processes. The influence of in-plane stresses of silicon plate with square, rectangular and circular shape have been investigated. The area of square, rectangular and circular form of elastic element has been approximated to be equal and the thickness is about 1μm. It was shown, that in-plane stresses can have a great influence on plate deflection and stresses distributions that should be taken into account at designing of piezoresistive pressure sensors. Finite element method (FEM) is adopted to optimize the sensor parameters, such as the membrane shape the deflection and stress caused by the different elastic membrane was analyzed to achieve higher sensitivity, larger full scale span and linearity.

Keywords: pressure sensor, elastic member, shape, defection, stress sensitivity, linearity, silicon.

1. INTRODUCTION

Silicon piezoresistive pressure sensors are used in various applications, which include automotive, aerospace and biomedical engineering. These sensors have small size, low power, good performance and mass production for the micro machined process. Design of micro piezoresistive pressure sensor extensively adopts finite element method (FEM) to realize stress distribution prediction, sensitivity enhancement and nonlinear reduction . In recent years substantial research has been carried out on micro machined, diaphragm-type pressure sensors [1-5]. The MEMS sensors are fabricated by different manufacturing technologies such as bulk-micromachining [6], [7] or surface-micromachining [8], [9]. Many of them use silicon and its piezoresistivity as the detection mechanism. These transducers function when the resistivity of the sensing resistor changes as the diaphragm deflects due to applied pressure. In order to increase the sensitivity, the diaphragms are made thinner so that the diaphragm has maximum deflection towards the input load. On the other hand, thin diaphragm under high pressure may result in large deflection and nonlinear effects that are not desirable. It is important to characterize the relationship between diaphragm thickness, deflection, and linearity, both analytically and experimentally in order to establish the design guidelines for MEMS pressure sensors. Square or rectangular plates are widely used as planar elastic element (EE) in piezoresistive and capacitive pressure sensors [10-12].Usually from the definition of deflection of mechanical member and to analyse the stresses in such elastic element a simplest model of elastic element is used. The elastic model is a thin silicon membrane. The thin silicon membrane is rigidly clamped plate and is loaded by cross-distributed loads of measured pressure. Usually for obtaining of numerical results the case of small deflection (w10.2h, w is the deflection and h is the thickness of elastic element) should be considered [13].In the more accurate model [14-15] the cross-distributed load takes into consideration as well as mechanical stresses in the plane of elastic element. These mechanical stresses arises due to two factors as follows:1. High level of impurity, which causes mechanical stresses in crystal lattice of silicon. 2. In plane forces, this acts on the side wall of the plate and causes mechanical stresses in silicon crystal lattice. However, even if simplest model is used, there are no analytical solutions. Thus, numerical methods, like finite element method (FEM), finite difference method (FDM) are widely used for finding the solution. The accuracy of result obtained depends on selection of initial functions for describing of deflections (shape functions) in the Elastic Element.

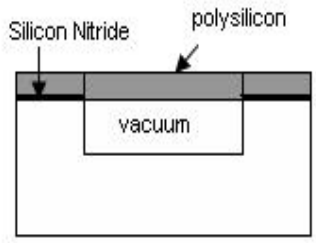

Figure-1. Pressure sensor.

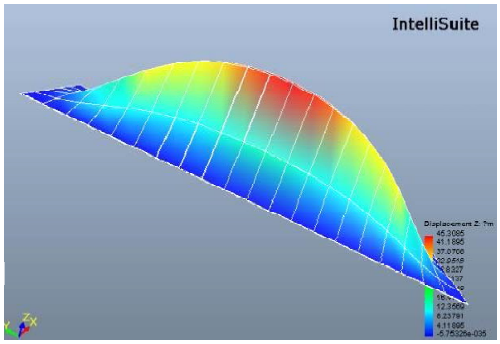

Figure-2. Displacement in case of rectangular diaphragm.

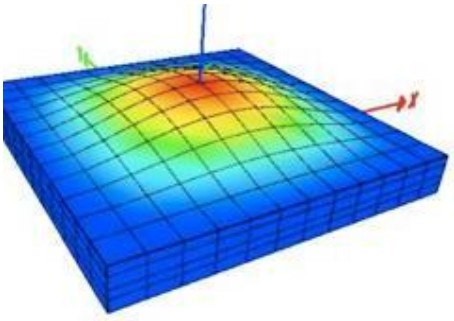

Figure-3. Displacement in case of square diaphragm.

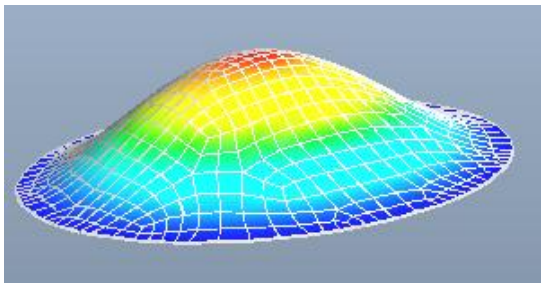

Figure-4. Displacement in case of circular diaphragm.

2. DESIGN OF ELASTIC MEMBER

The square, rectangular and circular-shape diaphragms have been designed, and characterized. Figure-2, Figure-3 and Figure-4 shows the deflection of the rectangular, square and circular diaphragm respectively. These pressure sensors are constructed with surface-micro machined diaphragms by a micromachining process which uses LPCVD sealing to create vacuum cavities [16]. The process starts with cleaning the wafer. A thin layer, 0.15 m, of LPCVD silicon nitride is then deposited. The cavity area is defined by a first mask via dry etching process to etch into the silicon of 1 m in depth. The wafer then goes through a thermal oxidation process to create about 2- m-thick silicon dioxide at the cavity area and to construct a flat surface LPCVD oxide of 0.5 m is then deposited to form the etch channels. These etch channels are defined by dry etching. The depth of the cavity is about 2 μm followed by a 1μm LPCVD polysilicon deposition, etch holes patterning (mask 3), and dry etching .The oxide in the etch channels and the cavity are now cleared by concentrated hydrofluoric acid (HF) etching. The second layer of polysilicon with 1μ m in thickness is then deposited by a second LPCVD polysilicon deposition step, which seals the etch holes and channels and creates a vacuum environment inside the cavity [17]. The size of the square diaphragm is 100 μm and the depth of the cavity is 2 μm and the thickness of the diaphragm is 1 μm.the circular diaphragm is also fabricated with the same procedure. Fig 1shows the cross sectional view of the fabricated pressure sensor. Times is specified, Times Roman or Times New Roman may be used. If neither is available on your word processor, please use the font closest in appearance to Times. Avoid using bit-mapped fonts. True Type 1 or Open Type fonts are required. Please embed all fonts, in particular symbol fonts, as well, for math, etc.

3. SENSITIVITY ANALYSIS

The sensitivity analyses are based on small deflection theories of plates. In classic mechanics, analytical solutions can be found for the pressure-deflection relationships of plates made of isotropic, homogeneous, linearly elastic materials [18]. Analytical models have been established for diaphragms with simple geometry such as square, rectangular, and circular shapes. For the case of circular-shape diaphragms under small deflection, the radial and circumferential strain with respect to the applied pressure can be derived as [18]

$$\epsilon_r = \frac{-3qa^2(1-v^2)}{8Eh^2}\left(1-\frac{3r^2}{a^2}\right) \quad (1)$$

$$\epsilon_\theta = \frac{-3qa^2(1-v^2)}{8Eh^2}\left(1-\frac{r^2}{a^2}\right) \quad (2)$$

Where E is the Young's modulus, q is the applied pressure, and υ is Poisson's ratio. The thickness of the diaphragm is represented as h and the radius as a. Subscripts r and Φ represent the radial and circumferential directions, respectively.

For the case of square-shape diaphragm under small deflection, a combination method suggested by Timoshenko is used in this paper [18]. It is assumed that the total deflection of a rectangular-shape plate with clamped edges is the summation of three components:ω_1, ω_2, and ω_3. The first component comes from the deflection of a simply supported plate under the same applied pressure. The second and third components are introduced to preserve the clamped boundary conditions. The following equations are derived for a rectangular plate with widths of a and b and bending stiffness D under an applied pressure q. The strain is solved. The circular-shape diaphragms are found to have similar characteristics as the square ones. In order to characterize the diaphragm, a program has been developed for both the square and circular diaphragms

$$\omega_1 = \frac{4qa^4}{D\pi^5}\sum_{m=odd}^{\infty}\frac{(-1)^{\frac{m-1}{2}}}{m^5}\cos\frac{m\pi x}{a} \left(1-\frac{(A_m tanhA_m+2)cosh\frac{m\pi y}{a}}{2coshA_m}+\frac{\frac{m\pi y}{a}sinh\frac{m\pi y}{a}}{2coshA_m}\right) \quad (3)$$

$$\omega_2 = \frac{-a^2}{2D\pi^2}\sum_{m=odd}^{\infty}\frac{E_m(-1)^{\frac{m-1}{2}}\cos\frac{m\pi x}{a}}{m^3coshA_m}\left(\frac{m\pi y}{a}sinh\frac{m\pi y}{a}-(A_m tanhA_m)cosh\frac{m\pi y}{a}\right) \quad (4)$$

$$\omega_3 = \frac{-b^2}{2D\pi^2}\sum_{m=odd}^{\infty}\frac{E_m(-1)^{\frac{m-1}{2}}\cos\frac{m\pi x}{b}}{m^3 cosh B_m} \quad (5)$$

$$\left(\frac{m\pi y}{b}sinh\frac{m\pi y}{b} - (B_m tanh B_m)cosh\frac{m\pi y}{b}\right)$$

Where

$$A_m = \frac{m\pi b}{2a} \quad (6)$$

$$B_m = \frac{m\pi a}{2b} \quad (7)$$

$$\omega = \omega_1 + \omega_2 + \omega_3 \quad (8)$$

$$\epsilon_{xx} = -z\frac{\partial^2\omega}{\partial x^2} \quad (9)$$

$$\epsilon_{yy} = -z\frac{\partial^2\omega}{\partial y^2} \quad (10)$$

$$\epsilon_{xy} = -2z\frac{\partial^2\omega}{\partial x\partial y} \quad (11)$$

4. RESULTS AND DISCUSSIONS

Finite element analysis was performed for the diaphragms of square, rectangular and circular shape with approximately equal area .The thickness of the diaphragm was about 1µm.The analysis was carried out in room temperature. The diaphragms with different shapes were subjected to a range of pressure from 0 to 35 MPa. Figure-5 shows the deflection of a square diaphragm. It has been seen that the deflection of the square diaphragm is nearly two times greater than the rectangular diaphragm displacement as shown in Figure-6.The pressure range of both the diaphragm is nearly equal. The Figure-7 shows the deflection of a circular diaphragm of radius 60 µm.

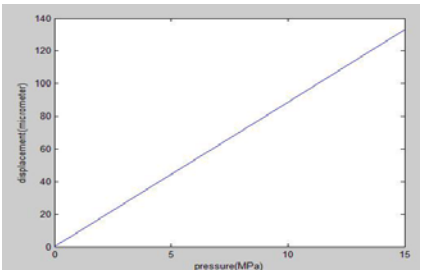

Figure-5. Displacement versus pressure for Square diaphragm with side 100 X 100µm.

The deflection is greater than the square diaphragm with sides 100 µm, but the pressure range of the circular diaphragm is 2MPa, which is small compared to the square diaphragm. Figure-8 shows the comparisons obtained between the different shapes of the diaphragm. The x-component, y-component and z-component stress analysis graph is shown in Figure-9, 10, 11 for square, rectangular and circular diaphragm respectively. It was found that the graph was linear for square and circular diaphragm. The y and z-component graph was non-linear for rectangular diaphragm. This is due to the non distribution of stress at the breath of the rectangle

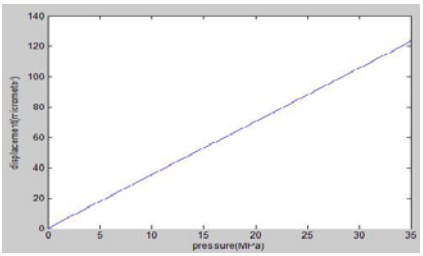

Figure-6. Displacement versus pressure for rectangular diaphragm with sides 110 x 90 µm.

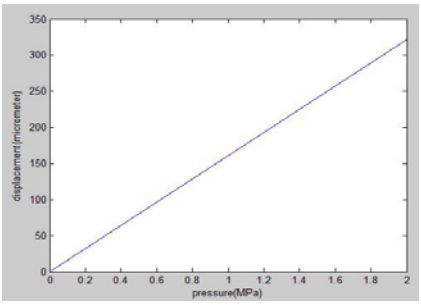

Figure-7. Displacement versus pressure for circular diaphragm with radius 60 µm.

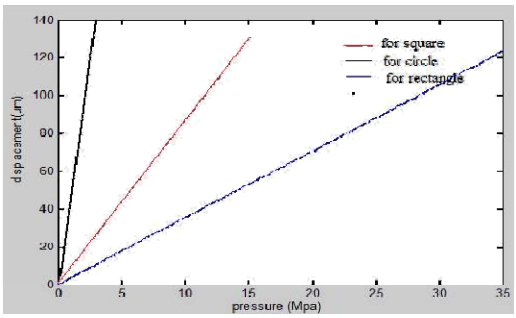

Figure-8. Displacement versus pressure for different shape diaphragm.

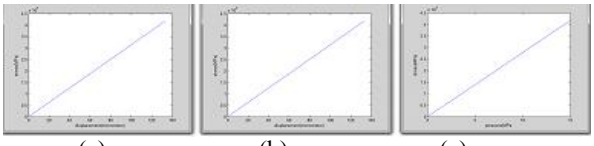

(a) (b) (c)

Figure-9. Stresses versus Displacement for Square diaphragm.

(a) x-component stress (b) y-component stress (c) z-component stress for square diaphragm

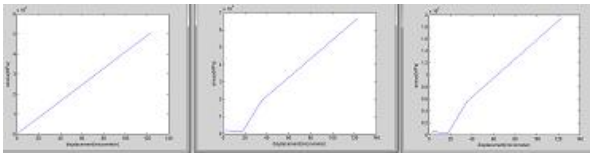

(a) (b) (c)

Figure-10. Stresses versus displacement for rectangular diaphragm.

(a) x-component stress (b) y-component stress (c) z-component stress for rectangular diaphragm

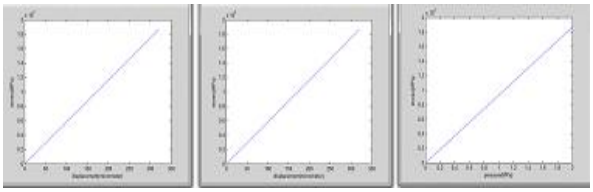

(a) (b) (c)

Figure-11. Stresses versus displacement for rectangular diaphragm.

(a) x-component stress (b) y-component stress (c) z-component stress for circular diaphragm

5. CONCLUSIONS

Finite element analysis is performed on the elastic element of the pressure sensor. The square, rectangle and circular shape of diaphragm of a pressure sensor was taken for analysis. It was found that the square and circular diaphragm gave good performance than the rectangular diaphragm. For low pressure range the circular diaphragm is best suited were as for high pressure range square diaphragm type pressure sensor is suitable.

REFERENCES

[1] W. H. Ko. 1986. Solid-state capacitive pressure transducers. Sens. Actuators. Vol. 10, pp. 303–320.

[2] H. L. Chau and K. D. Wise. 1987. Scaling limits in batch-fabricated sili-con pressure sensors. IEEE Trans. Electron Devices. Vol. ED- 34, pp. 850–858.

[3] K. Suzuki, S. Suwazono and T. Ishihara. 1987. Cmos integrated silicon pressure sensor. IEEE J. Solid-State Circuits. Vol. SSC-22, pp. 151– 156.

[4] J. T. Kung. and H.-S. Lee. 1992. An integrated air-gap-capacitor pressure sensor and digital readout with sub-100 attofarad resolution. IEEE J. Microelectromech. Syst. Vol. 1, pp.121–129.

[5] C. H. Mastrangelo, X. Zhang. and W. C. Tang. 1996. Surface-micromachined capacitive differential pressure sensor with lithographically defined silicon diaphragm. IEEE J. Microelectromech. Syst. Vol. 5, pp. 89–105.

[6] S. K. Clark. and K. D. Wise. 1979. Pressure sensitivity in anisotropically etched thin-diaphragm pressure sensors. IEEE Trans. Electron Devices. Vol. ED-26, pp. 1887–1896.

[7] Motorola Semiconductor Products Sector, Pressure sensors—Device Data, Phoenix, AZ, 1994.

[8] H. Guckel. 1991. Surface micromachined pressure transducers. Sens. Actuators. Vol. A28, pp. 133–146.

[9] S. Sugiyama., K. Shimaoka. and O. Tabata. 1991. Surface micromachined micro-diaphragm pressure sensors. In Proc. 6th Int. Conf. Solid-State Sensors and Actuators (Transducers'91). pp. 188–191.

[10] Peterson K. 1982. Silicon as a Mechanical Material, Proc. ZEEE, Vol.70, p. 420-457.

[11] Wu X. P. and Hu M.-F. *et al*. 1993. A Miniature Piezoresistive Catheter Pressure Sensor, Sensors and Actuators A. Vol. 35, pp. 197- 201.

[12] Timoshenko S. and Woinowsky-Kriger S. 1959. Theory of Plates and Shells, 2nd edn. N. Y: McGraw-Hill.

[13] S. teinmann R. Mechanical Behavior of Micromachined Sensor Membranes under Uniform External Pressure.

[14] Affected by In-plane Stresses Using a Ritz Method and Hermite Polynomials, Sensors and actuators, 1995, Vol. 48, p. 37-46.

[15] Schellin R. and Hess G. *et al*. 1994. Measurements of the Mechanical Behaviour of Micromachined Silicon and Silicon-nitride Membranes for Microphones, Pressure Sensors and Gas Flow\Meters, Sensors and Actuators A. Vol. 41-42, p. 287-292.

[16] W. Yun, L. Lin. and T. Haniff. 1998. Method of making a surface micro- machined silicon pressure sensors. U.S. Patent 5, pp. 759-870.

[17] L. Lin, K. M. McNair, R. T. Howe. and A. P. Pisano. 1993. Vacuum encapsulated lateral microresonators. In: Dig. Int. Conf. Solid- State Sensors and Actuators (Transducers'93). pp. 270– 273.

[18] Shells, 2nd ed. 1970. New York: McGraw-Hill.